Electronic supplementary information (ESI) for Chemical Communications

From nano- to macro-engineering of oxide-encapsulated-nanoparticles for harsh reactions: One-step organization via cross-linking molecules

Qiaofei Zhang,‡[a] Guofeng Zhao,‡*[a] Zhiqiang Zhang,[a] Lupeng Han,[a] Songyu Fan,[a] Ruijuan Chai,[a]

Yakun Li,[a] Ye Liu,[a] Jun Huang[b] and Yong Lu*[a]

[a] Shanghai Key Laboratory of Green Chemistry and Chemical Processes, School of Chemistry and

Molecular Engineering, East China Normal University, Shanghai, 200062, China

[b] School of Chemical and Biomolecular Engineering, University of Sydney, NSW 2006, Australia

* To whom correspondence should be addressed

Tel. & Fax: (+86)21-62233424

E-mail: *gfzhao@chem.ecnu.edu.cn* (G. Zhao)*; ylu@chem.ecnu.edu.cn* (Y. Lu)

‡ Q.Z. and G.Z. contributed equally to this work.

Materials and Methods

Catalyst preparation

Synthesis of microfibrous structured AlOOH/Al-fiber substrate

The synthesis of microfibrous structured AlOOH/Al-fiber substrate was described in details in the previous publication.[S1] Briefly, the 3 dimensional (3D) Al-fiber network consisting of 10 vol% 60 μm Al-fiber (99.9 wt% purity) and 90 vol% voidage was utilized as the substrate (purchased from Shanghai Xincai Net-structured Material Co. Ltd., China). The typical preparation of such unique AlOOH/Al-fiber substrate involved two simple steps: circular chips punched down from their large felt were ultrasonically degreased in acetone for 10 min and etched in 10 mL NaOH (0.1 wt%) aqueous solution for 2 min to remove original barrier oxide layer and thoroughly washed using deionized water; the pretreated chips were packed layer-by-layer into a quartz tube and treated in water steam flow at 120 °C for 6 h for steam-only oxidation of Al ($2Al + 4H_2O = 2AlOOH + 3H_2$). After dried at 120 °C for 2 h in N_2 flow, microfibrous structured AlOOH/Al-fiber substrate was obtained.

Synthesis of monolithic structured Ni(OH)$_2$/Ni-foam substrate

The synthesis of monolithic Ni(OH)$_2$/Ni-foam substrate was prepared by a facile hydrothermal method. Firstly, Ni-foam wafers (2 mm thick, diameter of 8 mm, 100 pores per inch; purchased from Changsha Lyrun Material Co., Ltd, China) were cut from their large mother-sheet and then ultrasonically degreased in acetone for 10 min. Typically, the 0.01 M Ni(NO$_3$)$_2$ and 0.04 M NH$_4$Cl aqueous solution were prepared with specified amount of hexahydrate Ni(NO$_3$)$_2$ and NH$_4$Cl dissolved in distilled water under stirring for 30 min at room temperature. Subsequently, 0.5 g of

cleaned Ni-foam was immersed into the 80 mL above mentioned homogenous solution and then the Ni-foam and solution were sealed inside a Teflon-lined stainless steel autoclave at 100 °C for 3 h.

Synthesis of microfibrous structured Pd/Al$_2$O$_3$/Al-fiber catalyst

The microfibrous structured Pd/Al$_2$O$_3$/Al-fiber catalyst was prepared by solvent-assistant incipient wetness impregnation with an acetone solution of palladium acetate (Pd(Ac)$_2$). The as-prepared AlOOH/Al-fiber substrate was directly impregnated with Pd(Ac)$_2$ solution, followed by dried at 100 °C and calcined at 300 °C in air for 2 h to obtain the Pd/Al$_2$O$_3$/Al-fiber catalyst (actual Pd-loading of 0.3 wt%).

Synthesis of microfibrous structured Pd@SiO$_2$/Al$_2$O$_3$/Al-fiber catalyst

The microfibrous structured Pd@SiO$_2$/Al$_2$O$_3$/Al-fiber catalyst was prepared by one-pot self-assembly method with the aid of cross-linking molecule 3-aminopropyltriethoxysilane (APTES). A certain amount of Pd(Ac)$_2$ was firstly dissolved in the acetone, forming an orange-color solution. Then APTES was added into the solution with a molar ratio of Pd: APTES of 1: 3, and the solution color was transformed to faint yellow spontaneously, indicating the formation of Pd^{2+}-APTES complexes. When the AlOOH/Al-fiber substrate was added into the solution of Pd^{2+}-APTES complexes in an incipient impregnation manner, the silanisation reaction took place between the ethoxy (-O-CH$_2$-CH$_3$) groups of APTES and the surface hydroxyl (-OH) groups of AlOOH nanoarrays with leaving of ethanol, leading to the formation of Al-O-Si bonds. After 4 h, the Pd^{2+}-APTES-grafted AlOOH/Al-fiber was obtained. Subsequently, some water was added into the system, and the rest -Si-O-CH$_2$-CH$_3$ polymerized with the aid of the added water to produce Si-O-Si bonds. Followed by dried at 100 °C for 2 h and calcined at 550 °C for 3 h in air as well as at

150 $^{\circ}$C for 2 h in H$_2$, the microfibrous structured Pd@SiO$_2$/Al$_2$O$_3$/Al-fiber catalyst could be obtained.

Synthesis of microfibrous structured NiO@TiO$_2$/Al$_2$O$_3$/Al-fiber catalyst

The microfibrous structured NiO@TiO$_2$/Al$_2$O$_3$/Al-fiber catalyst was prepared by one-pot self-assembly method with the aid of cross-linking molecule titanium(IV) bis(triethanolaminate) diisoproxide (TBTAD). A certain amount of Ni(NO$_3$)$_2$ was firstly dissolved in the ethanol, forming a green-color solution. Then TBTAD was added into the solution with a molar ratio of Ni: TBTAD of 3: 1, and the solution color was transformed to faint green spontaneously, indicating the formation of Ni^{2+}-TBTAD complexes. When the AlOOH/Al-fiber substrate was added into the solution of Ni^{2+}-TBTAD complexes in an incipient impregnation manner, the reaction took place between the isoproxide groups of TBTAD and the surface hydroxyl (-OH) groups of AlOOH nanoarrays with leaving of isopropanol, leading to the formation of Al-O-Ti bonds. After 4 h, the Ni^{2+}-TBTAD-grafted AlOOH/Al-fiber was obtained. Subsequently, some water was added into the system, and Ti-O-Ti bonds were produced. Followed by dried at 100 $^{\circ}$C for 12 h and calcined at 450 $^{\circ}$C for 3 h in air, the microfibrous structured NiO@TiO$_2$/Al$_2$O$_3$/Al-fiber catalyst could be obtained.

Synthesis of monolithic structured Cu@ZrO$_2$/NiO/Ni-foam catalyst

The monolithic Cu@ZrO$_2$/NiO/Ni-foam catalyst was prepared by one-pot self-assembly method with the aid of zirconium coupling agent (OC-6-22)-tris(3-aminophenolato-kappa-O)2,2-bis(2-propenyloxy-kappa-O)methyl-1-butanolato-kappa-O-zirconium (TAPBPMBZ). A certain amount of anhydrous Cu(NO$_3$)$_2$ ethanol solution was

added into the zirconium coupling agent ethanol solution with a 10 wt% Cu and 1 wt% TAPBPMBZ on the basis of the weight of $Ni(OH)_2$/Ni-foam substrate, forming a dark-gray solution. The $Ni(OH)_2$/Ni-foam substrate was added into the solution of Cu^{2+}-TAPBPMBZ complexes in an incipient impregnation manner and the Cu^{2+}-TAPBPMBZ-grafted $Ni(OH)_2$/Ni-foam was obtained. Subsequently, some water was added into the system, and Zr-O-Zr bonds were produced. Followed by dried at 100 ^{o}C for 8 h and calcined at 300 ^{o}C for 2 h in air as well as at 250 ^{o}C for 4 h in H_2, the monolithic $Cu@ZrO_2/NiO$/Ni-foam catalyst could be obtained.

Synthesis of microfibrous structured Au(or AuCu)@SiO₂/Al₂O₃/Al-fiber catalyst

The microfibrous structured $Au@SiO_2/Al_2O_3$/Al-fiber catalyst was prepared by one-pot self-assembly method with the aid of APTES. A certain amount of $AuCl_3$ was directly dissolved in APTES with a molar ratio of Au: APTES of 1: 6, forming an orange-color solution. When the AlOOH/Al-fiber substrate was added into the solution of Au^{3+}-APTES complexes in an incipient impregnation manner, the silanisation reaction took place between the ethoxy ($-O-CH_2-CH_3$) groups of APTES and the surface hydroxyl (-OH) groups of AlOOH nanoarrays with leaving of ethanol, leading to the formation of Al-O-Si bonds. After 4 h, the Au^{3+}-APTES-grafted AlOOH/Al-fiber was obtained. Subsequently, some water was added into the system, and the rest $-Si-O-CH_2-CH_3$ polymerized with the aid of the added water to produce Si-O-Si bonds. Followed by dried at 100 ^{o}C for 2 h and calcined at 550 ^{o}C for 3 h in air as well as at 300 ^{o}C for 2 h in H_2, the microfibrous structured $Au@SiO_2/Al_2O_3$/Al-fiber catalyst could be obtained. The same procedures were conducted to synthesize the $AuCu_4@SiO_2/Al_2O_3$/Al-fiber catalyst.

Catalyst characterization

The actual loadings of metals in all samples were determined via washing the samples in aqua regia solution and measuring the metal ion concentrations in the leached solutions by inductively coupled plasma-atomic emission spectroscopy (ICP-AES; ICP Thermo IRIS Intrepid II XSP; USA). The surface morphology and cross-sectional structure of the samples were visualized by scanning electron microscope (SEM; Hitachi S-4800; Japan). The nano-scaled structure of the catalysts and the size of metal nanoparticles (MNPs) were characterized by transmission electron microscope (TEM; FEI-Tecnai G2F30; USA) operated at 300 kV. X-ray diffraction (XRD) patterns of the samples were conducted on a Rigaku Ultra IV diffractometer (Japan) with Cu Kα radiation (λ = 0.1542 nm) at 35 kV and 25 mA in the 2θ scanning range of 5-90° at the scanning rate of 10 ^{o} min^{-1}. The porous structure of the samples were characterized by N_2 adsorption-desorption isotherms at liquid nitrogen temperature using a Quantachrome Autosorb-3B system (USA), and surface area, pore size distribution and total pore volume was analyzed by Brunauer-Emmett-Teller (BET) and Barrett-Joyner-Halenda (BJH) methods. The metal dispersion and size were also calculated based on CO pulse chemisorption experiments obtained at 20 ^{o}C after in-situ reducing the samples in H_2 at 150 ^{o}C for 2 h followed by purging in a He flow for 1 h (Quantachrome ChemBET-3000; USA). Fourier transform infrared spectroscopy (FTIR) experiments were performed on a Nicolet Nexus 670 spectrometer (USA) equipped with a liquid-nitrogen cooled mercury cadmium telluride (MCT) detector by taking 512 scans at a resolution of 4 cm^{-1}. The magic-angle spinning nuclear magnetic resonance (MAS-NMR) spectra of ^{27}Al were measured on a VARIAN VNMRS 400 WB NMR spectrometer.

Reactivity tests

Catalytic combustion of CH₄ and VOCs

The catalytic combustion of CH_4 and VOCs was conducted in a fixed-bed tubular quartz reactor (600 mm length and 8 mm inner diameter) under atmospheric pressure without any pretreatment of the catalyst. A gaseous mixture of 1 vol% CH_4 in air or 1,000 ppm single VOC in air was employed as feedstock with gas hourly space velocity (GHSV) of 72,000 mL g^{-1} h^{-1}, if not specified. Circular chips (8.1 mm diameter) of the microfibrous structured catalysts (0.15 g) were packed layer-up-layer into the tube reactor. Three calibrated mass flow controllers were used to control the CH_4, O_2 and N_2 gas. The product effluent was analyzed online by an HP 6850 gas chromatograph equipped with a TCD connected to Plot Q and MS 5A parallel capillary columns (DIKMA). The gas pipeline and sampling 6-way valve between the reactor outlet and the GC injector were heated to ensure the effluent completely evaporated. The catalyst activity was defined by T_{10}, T_{50} and T_{90}, representing the reaction temperatures for the CH_4 (or VOC) conversion of 10%, 50% and 90%, respectively.

Oxidative dehydrogenation of ethane to ethene (ODE)

The ODE with molecular oxygen was performed on a fixed-bed tubular quartz reactor (600 mm length and 8 mm inner diameter) at 450 °C under atmospheric pressure without any pretreatment of catalyst. A gaseous mixture of 10% C_2H_6, 10% O_2 and 80% N_2 was used with gas hourly space velocity (GHSV) of 9,000 mL g^{-1} h^{-1}, if not specified. Circular chips (8.1 mm diameter) of the microfibrous structured catalysts (0.2 g) were packed layer-up-layer into the tube reactor. Three calibrated mass flow controllers were used to control the C_2H_6, O_2 and N_2 gas. The product effluent was analyzed online by an HP 6850 gas chromatograph equipped with a TCD connected to Plot U

and MS 5A parallel capillary columns (DIKMA). CO_2, C_2H_4 and C_2H_6 were quantified online by Plot U column and O_2, CH_4 and CO were quantified by 5A molecular sieve column. The gas pipeline and sampling 6-way valve between the reactor outlet and the GC injector were heated to ensure the effluent completely evaporated.

Gas-phase hydrogenation of dimethyl oxalate (DMO)

The DMO hydrogenation was performed in a fixed-bed stainless-steel reactor with 8 mm inner diameter. Firstly 0.5 g catalyst was loaded into reactor and heated to 230 °C, and then pure hydrogen was introduced to the reactor until the pressure was raised to 2.5 MPa and DMO methanol solution (13 wt%) was simultaneously introduced to the reactor at a weight hourly space velocity (WHSV) of 5.1 h^{-1}. WHSV was calculated by dividing the mass flow rate of DMO methanol solution by the catalyst mass. The DMO methanol solution was pumped using high-pressure advection pump and the liquid products was collected and analyzed using a Shimadzu 2014C gas chromatography-flame ionization detector (GC-FID) with a HP-INNOWax column.

Gas-phase selective oxidation of benzyl alcohol

The gas-phase selective oxidation of benzyl alcohol on the $Au@SiO_2/Al_2O_3/Al$-fiber and $AuCu_4@SiO_2/Al_2O_3/Al$-fiber catalysts was performed on a fixed-bed quartz tube reactor (600 mm length by 16 mm inner diameter) at 270 °C under atmospheric pressure as described previously.[S2] The catalyst used in test experiments was 0.5 g if not specifically noted. Benzyl alcohol was continuously fed with the speed of 2 g/h using a high-performance liquid pump in parallel with O_2 (oxidant of 4.5 ml/min) and N_2 (diluted gas of 50 mL/min) feeding using calibrated mass flow controllers into the reactor. WHSV was calculated by dividing the mass flow rate of alcohol

feedstock by the catalyst mass. The effluent was cooled using an ice-salt bath (-15 $^\circ$C) to liquefy the condensable vapours for analysis using an Shimadzu-2014 GC gas chromatography-flame ionization detector (GC-FID) with a 60 m HP-5ms capillary column. The gas-phase products, such as H_2, CO_x, and C1-C3 hydrocarbons, were analyzed using an HP-5890 GC with a TCD and a 30 m AT-plot 300 capillary column. The stability test was conducted at 270 $^\circ$C.

TOF calculations

In order to assess the intrinsic activity, so called turnover frequency (TOF, here defined as the quantity of CO_2 produced per surface Pd atom per hour) was calculated. The quantity of CO_2 formed per unit time (mol s^{-1}) could be obtained by dividing the molar volume of gas (V_m, L mol^{-1}, assuming ideal behavior at 25 $^\circ$C) into the flow of CH_4 (F, L s^{-1}) times α (the yield of CO_2). The number (N, mol g^{-1}) of active sites (*i.e.*, surface Pd atoms) was determined by CO pulse chemisorption. In accordance, the TOF could be calculated by:

$$\text{TOF} = \frac{\text{Product Molecules}}{\text{Active Sites} \cdot \text{Time}} = \frac{F \cdot \alpha}{V_m \cdot N}.$$

The CH_4 conversion was retained at below 10% by tuning the GHSV for the TOF calculations. As an example, the TOF of the Pd/Al$_2$O$_3$/Al-fiber was calculated as following. The flow of CH_4 gas (F) was set to 1.5 mL min^{-1}. At 260 $^\circ$C, about 6.4% of CH_4 was converted into CO_2 over 0.15 g catalyst with 100% CO_2 selectivity for a feedgas of 1 vol% CH_4 in air at total GHSV of 60,000 mL g^{-1} h^{-1}, and thus the yield of CO_2 (*i.e.*, α) accounted to 6.4%. The molar amount of surface Pd per gram catalyst of Pd/Al$_2$O$_3$/Al-fiber was determined to be 1.6×10^{-5} mol g^{-1} by CO chemisorption. It

was supposed that every surface Pd atom was an active site, the TOF of Pd/Al$_2$O$_3$/Al-fiber could thus be calculated as:

$$\text{TOF} = \frac{\frac{1.5}{1000 \cdot 60} \ (\text{L s}^{-1}) \cdot 0.064}{24.8 \ (\text{L mol}^{-1}) \cdot 1.6 \cdot 10^{-5} \ (\text{mol g}^{-1}) \cdot 0.15 \ (\text{g})} = 0.027 \ \text{s}^{-1} = 97 \ \text{h}^{-1}$$
.

Analysis of FTIR and Al-NMR spectra

FTIR in Fig. 1B shows the characteristic vibrational peak of Pd-N appearing at 613 cm^{-1}, which confirms the formation of Pd^{2+}-APTES chelates.[S3] Al-NMR in Fig. 1C shows a new resonance at 68 ppm assigning to the tetrahedral aluminum (Al^{IV}), indicating the generation of Al-O-Si bond.[S4] The cross-linking of silicon groups was confirmed by FTIR in Fig. 1D. The original easily-distinguishable sharp bands of Si-O-C stretching vibration at 958, 1080 and 1103 cm^{-1} were transformed into two broad stretching bands of Si-O-Si.[S5]

Table S1. Catalyst characteristics and TOFs for CH_4 combustion catalyzed by the microfibrous structured Pd/Al$_2$O$_3$/Al-fiber and Pd@SiO$_2$/Al$_2$O$_3$/Al-fiber catalysts.

Catalyst	Pd loading	S_{BET}	$T_{10}{}^b$	$T_{50}{}^b$	$T_{90}{}^b$	Surf. Pd^c	Pd size^c	TOF^d
	(wt%)^a	(m^2 g^{-1})	(°C)	(°C)	(°C)	(mol g^{-1})	(nm)	(h^{-1})
Pd/Al$_2$O$_3$/Al-fiber	0.3	15	270	324	360	1.6×10^{-5}	2.0	97
Pd/Al$_2$O$_3$/Al-fiber^e	0.3	8	—	—	—	4.5×10^{-6}	7.1	89
Pd@SiO$_2$/Al$_2$O$_3$/Al-fiber	0.3	25	275	325	365	1.4×10^{-5}	2.3	78
Pd@SiO$_2$/Al$_2$O$_3$/Al-fiber^f	0.3	24	—	—	—	1.3×10^{-5}	2.4	80

^{a} Measured by ICP-AES. ^{b} T_{10}, T_{50} and T_{90} represent the reaction temperatures for the CH_4 conversion of 10%, 50% and 90%, respectively (0.15 g Cat., 1 vol% CH_4 in air, GHSV = 72,000 mL $g_{cat.}^{-1}$ h^{-1}). ^{c} Determined by CO pulse absorption. ^{d} TOF at 260 °C based on CO_2 yield and surface Pd. ^{e} The Pd/Al$_2$O$_3$/Al-fiber catalyst after 400-h test. ^{f} The Pd@SiO$_2$/Al$_2$O$_3$/Al-fiber catalyst after 1,000-h test.
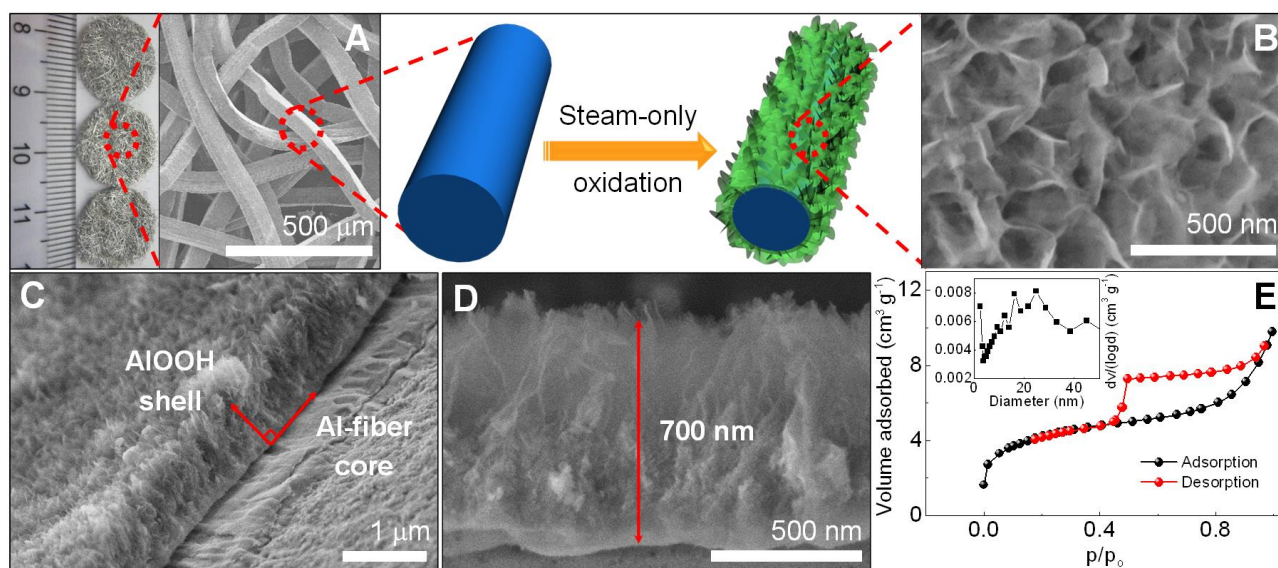
Fig. S1. (A) Photograph of macroscopic samples (left) and low-magnification SEM image (right) of the original thin-sheet Al-fiber with open 3D macroporous network. (B) High-magnification SEM image of AlOOH/Al-fiber substrate prepared by steam-only oxidation at 120 °C for 6 h, showing a honeycomb-like morphology of AlOOH nanoarrays. (C,D) SEM images of AlOOH/Al-fiber with AlOOH layer covering Al-fiber. (E) N$_2$ adsorption-desorption isotherms of AlOOH/Al-fiber (inset: Barrett-Jovner-Halenda (BJH) mesopore size distribution calculated on the basis of adsorption branch). Note that the AlOOH/Al-fiber substrate presented a much higher specific surface area (SSA) of 15-17 m^2 g^{-1} than of the original Al-fiber substrate (~1 m^2 g^{-1}). The detailed information of AlOOH/Al-fiber structure could be found in Ref S1.
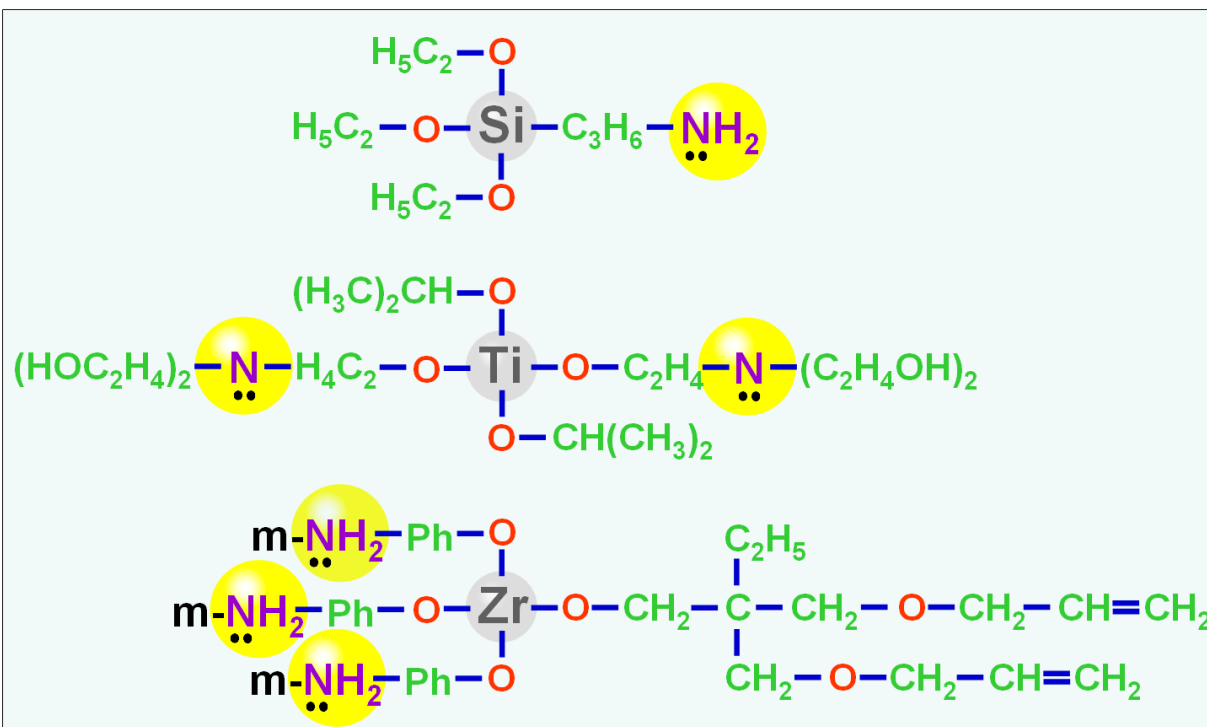
Fig. S2. The cross-linking molecules. Upper: 3-aminopropyltriethoxysilane (APTES); Middle: titanium(IV) bis(triethanolaminate) diisoproxide (TBTAD). Lower: (OC-6-22)-tris(3-aminophenolato-kappa-O)2,2-bis(2-propenyloxy-kappa-O)methyl-1-butanolato-kappa-O-zirconium (TAPBPMBZ).
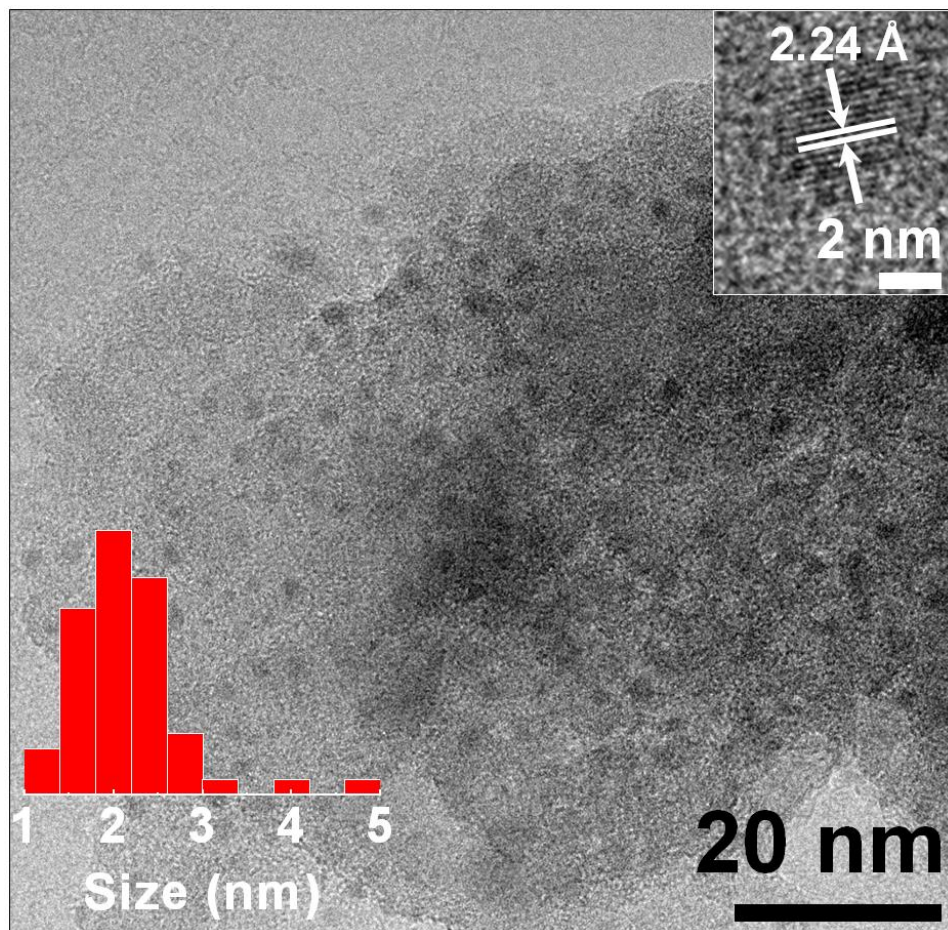
Fig. S3. TEM images of the fresh Pd@SiO$_2$/Al$_2$O$_3$/Al-fiber (0.3 wt% Pd-loading) catalyst with corresponding particle size distribution histogram as well as the lattice distance of 0.224 nm corresponding to Pd(111) facet.
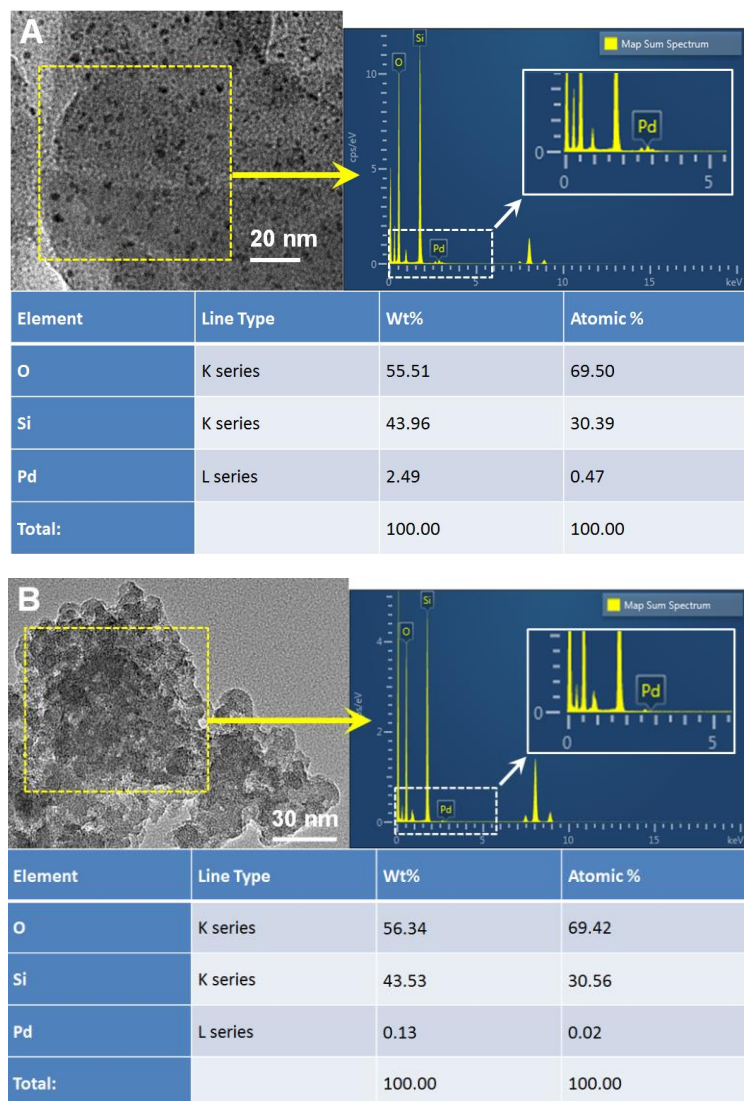
A

Element	Line Type	Wt%	Atomic %
O	K series	55.51	69.50
Si	K series	43.96	30.39
Pd	L series	2.49	0.47
Total:		100.00	100.00

B

Element	Line Type	Wt%	Atomic %
O	K series	56.34	69.42
Si	K series	43.53	30.56
Pd	L series	0.13	0.02
Total:		100.00	100.00

Fig. S4. TEM-EDS analysis of the Pd@SiO$_2$/Al$_2$O$_3$/Al-fiber (Pd loading of 0.3 wt%) sample before (A) and after (B) the treatment of HNO$_3$ solution.

Note: The real Pd loading in the Pd@SiO$_2$/Al$_2$O$_3$/Al-fiber catalyst is 0.3 wt%. After HNO$_3$-solution treatment, the Al-fiber and Al$_2$O$_3$ was removed and it is hard to compare the changes in Pd loadings before and after treatment if with containing Al-fiber and Al$_2$O$_3$. Therefore, the Pd loading was analyzed just with containing SiO$_2$, and the EDS Pd-loading of the untreated sample is 2.49 wt%, much higher than its real loading of 0.3 wt%.
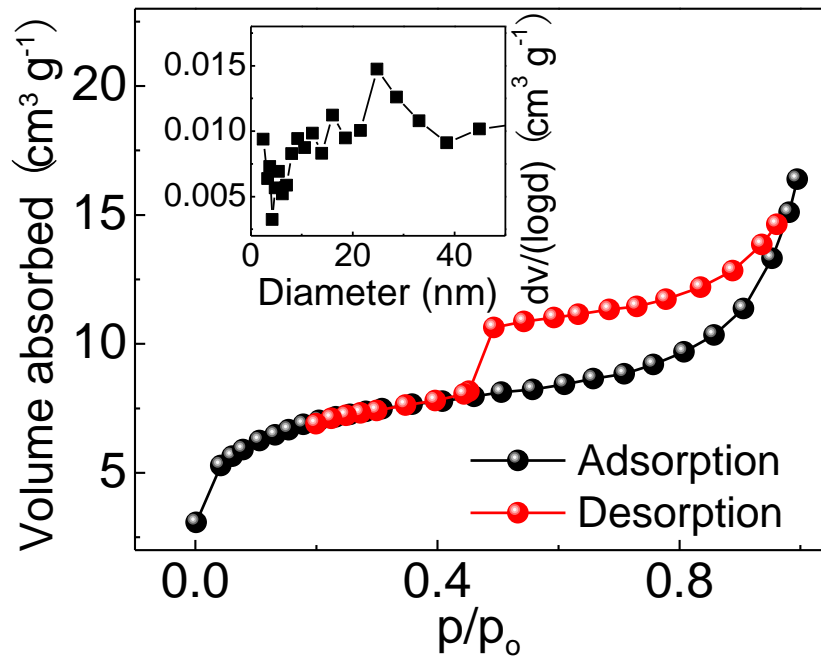
Fig. S5. N_2 adsorption-desorption isotherms (inset: Barrett-Jovner-Halenda (BJH) mesopore size distribution calculated by the adsorption branch) of the fresh Pd@SiO_2/Al_2O_3/Al-fiber catalyst.
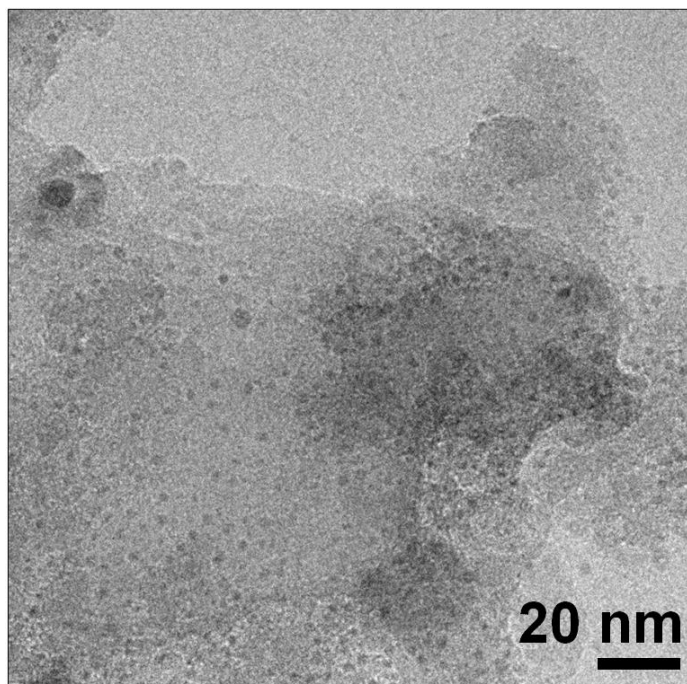
Fig. S6. TEM image of the Pd@SiO$_2$/Al$_2$O$_3$/Al-fiber (0.3 wt% Pd-loading) catalyst heated in air at 550 ^{o}C for 2 h.
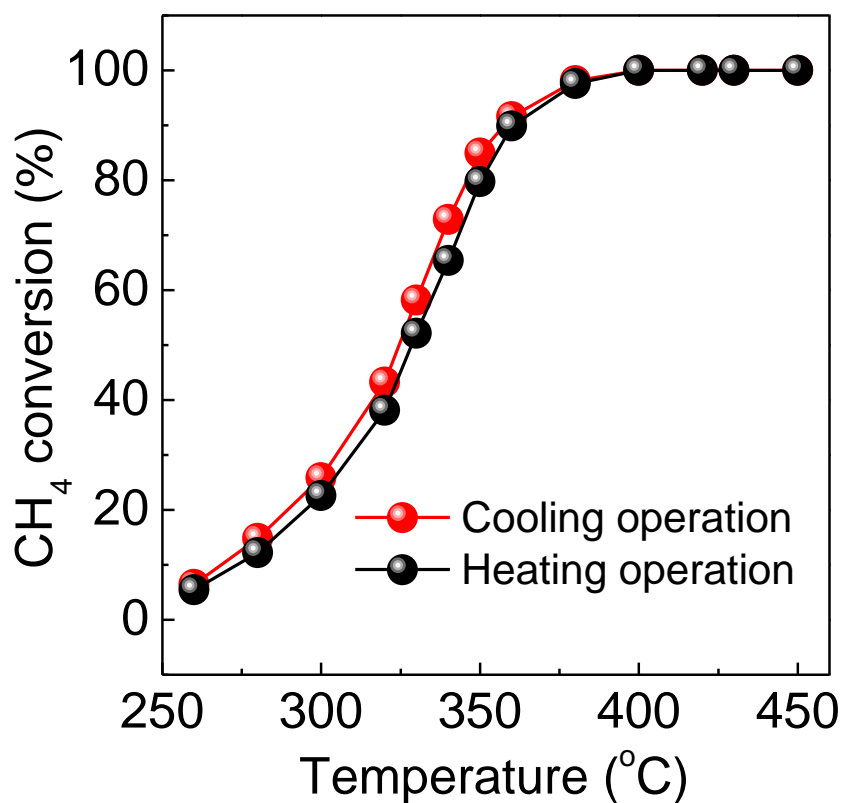
Fig. S7. CH_4 conversion against reaction temperature for the heating and cooling operations over the Pd@SiO_2/Al_2O_3/Al-fiber (0.3 wt% Pd-loading) catalyst. Reaction conditions: 1 vol% CH_4 in air, GHSV = 72,000 mL $g_{cat.}^{-1}$ h^{-1}.

Note: The CH_4 conversions for the cooling operation (*i.e.* reaction temperature cooling from 450 to 260 ^{o}C) is very close to the ones for the heating operation (*i.e.* reaction temperature heating from 260 to 450 ^{o}C). These results indicate that in the cooling operation process the reaction heat (produced at the former higher reaction temperature) isn't trapped, which would make a higher CH_4 conversion at the followed lower temperature otherwise, due to the high thermal conductivity of our catalyst.
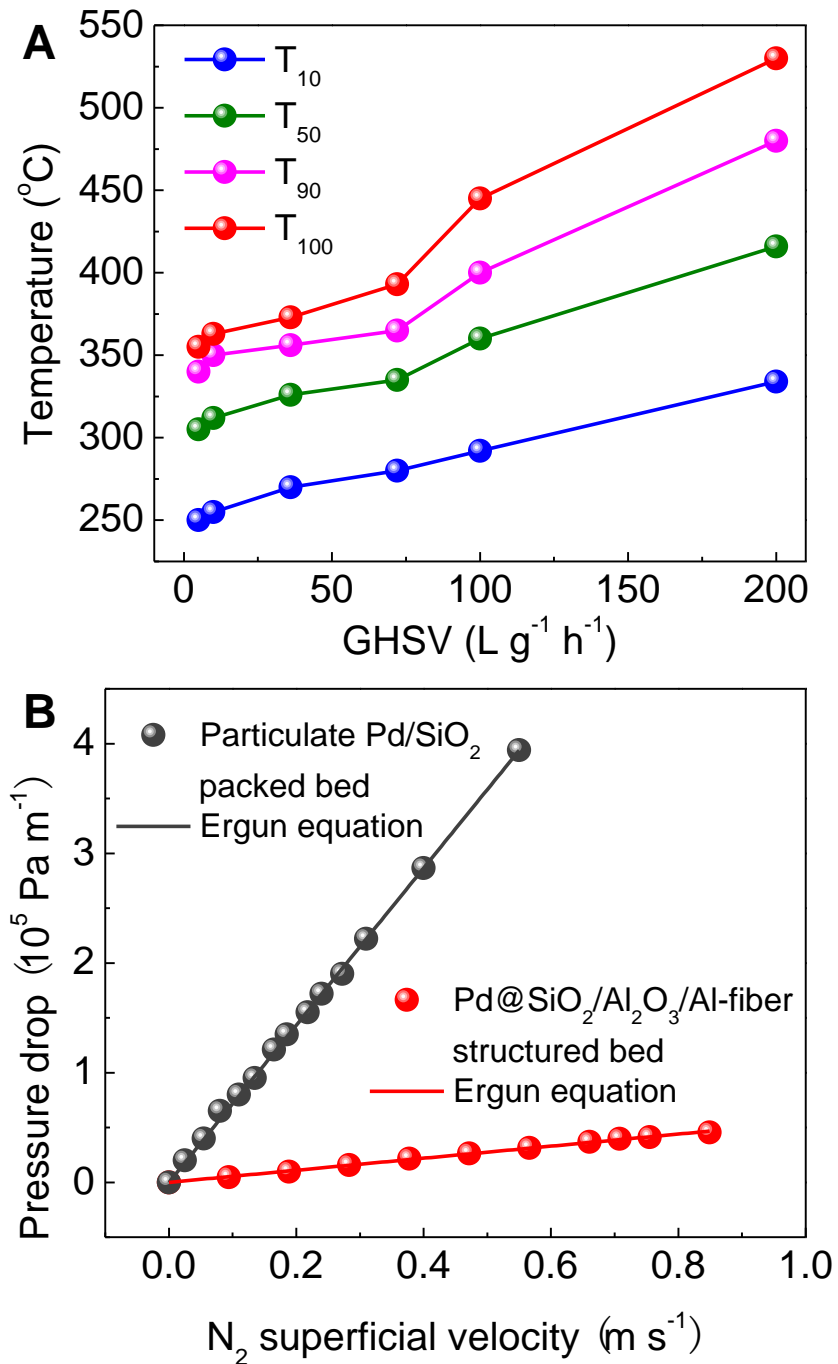
Fig. S8. (A) Effect of GHSV on the performance of the Pd@SiO₂/Al₂O₃/Al-fiber (0.3 wt%

Pd-loading) for CH₄ combustion. Reaction conditions: 1 vol. % CH₄ in air. (B) Profiles of pressure

drop per meter as a function of N₂ superficial velocity over monolithic Pd@SiO₂/Al₂O₃/Al-fiber

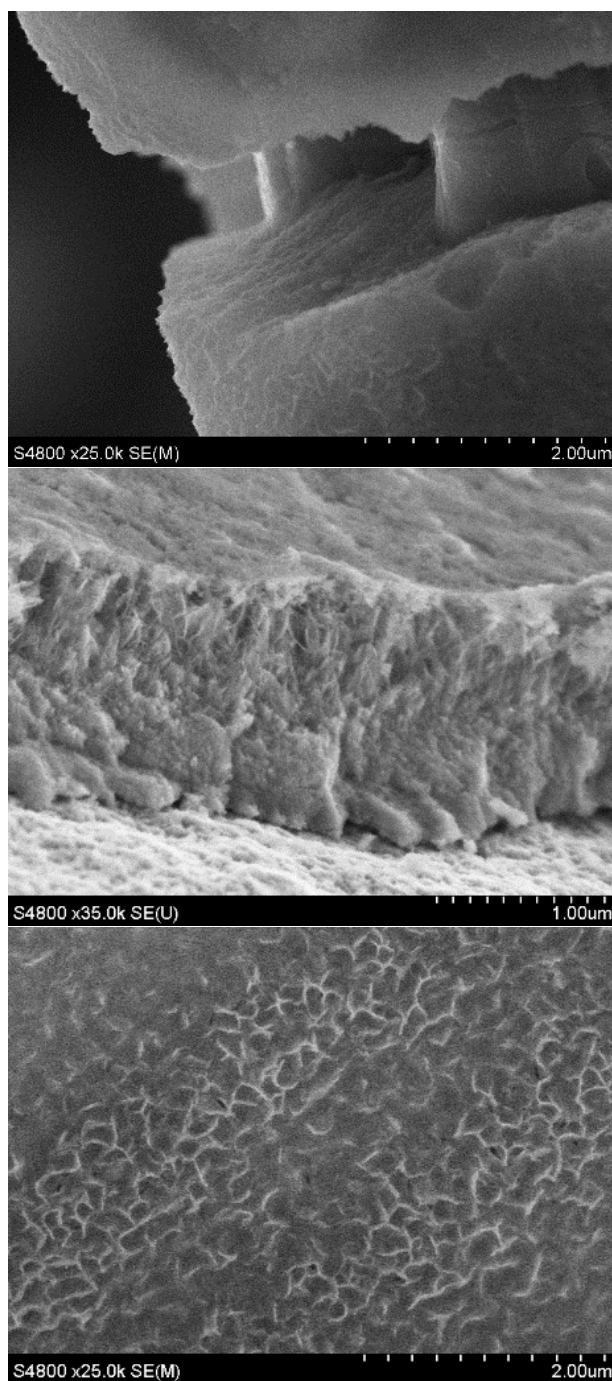structured bed and particulate Pd/SiO₂ (0.2 mm) packed bed.

Fig. S9. SEM images of the Pd@SiO$_2$/Al$_2$O$_3$/Al-fiber (0.3 wt% Pd-loading) catalyst after 1,000-h test. Reaction conditions: 350 $^{\circ}$C and 72,000 mL·g$_{cat.}^{-1}$·h^{-1} for 200 h; subsequently 380 $^{\circ}$C and 36,000 mL·g$_{cat.}^{-1}$·h^{-1} for the next 800-h.
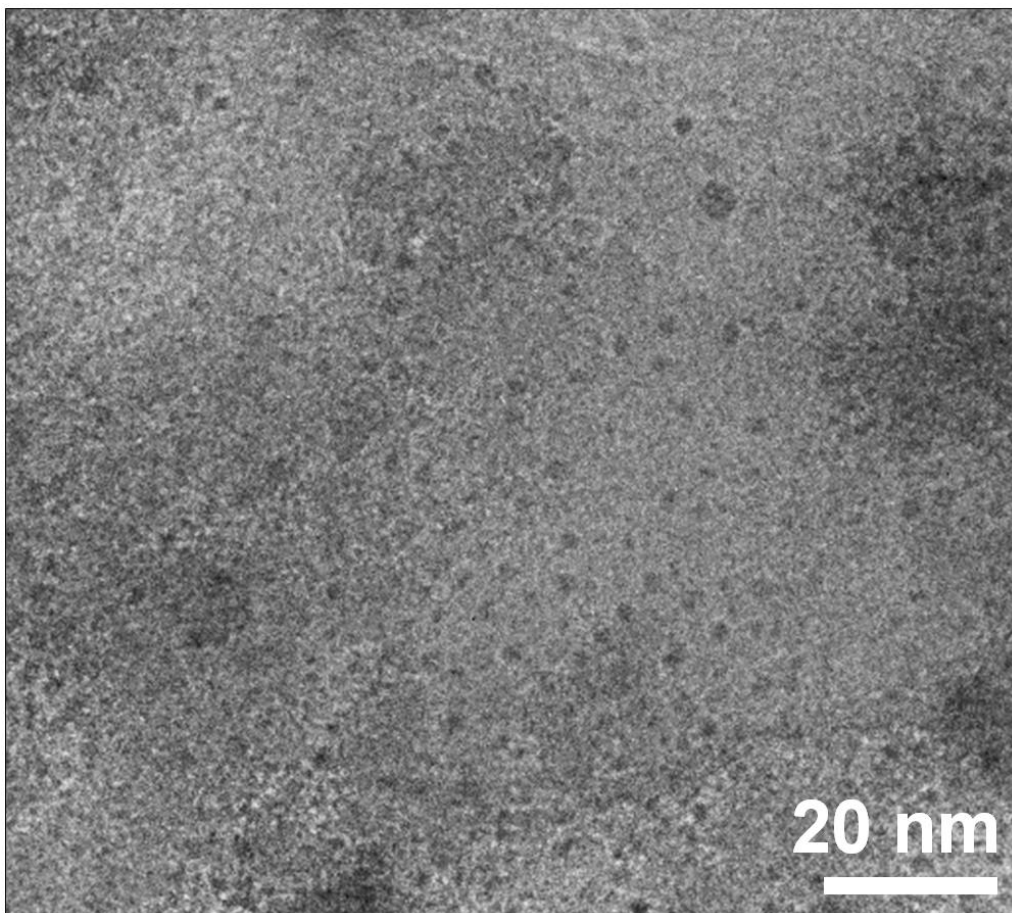
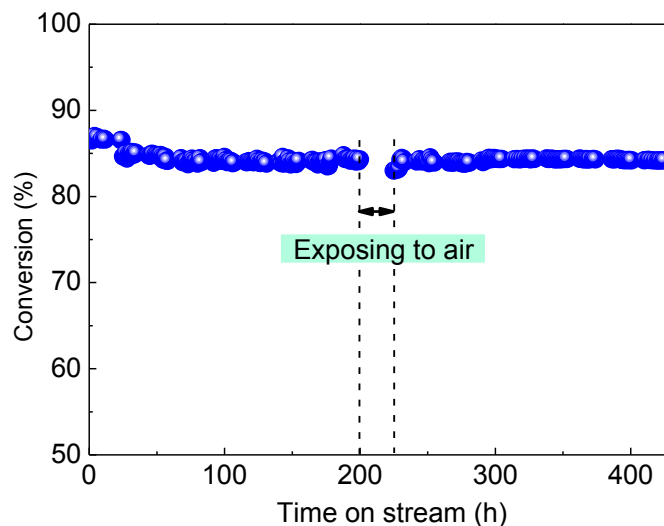**Fig. S10.** TEM image of the fresh Pd/Al$_2$O$_3$/Al-fiber (0.3 wt% Pd-loading) catalyst with Pd size of 2-3 nm.

Fig. S11. Stability test of the Pd@SiO_2/Al_2O_3/Al-fiber (Pd-loading of 0.3 wt%) for CH_4 combustion with an operation breaking by exposing the catalyst to air for 24 h. Reaction conditions: 1 vol% CH_4 in air, 350 $^{\circ}$C, GHSV = 36,000 mL $g_{cat.}^{-1}$ h^{-1}.

Note: The catalyst demonstrated high stability within the first 200-h running. To further investigate the reusability, the catalyst was exposed to the air for 24 h after its first running. Then the catalyst was further performed another 200-h running under the same conditions, showing excellent reusability with CH_4 conversion retained at 84%.
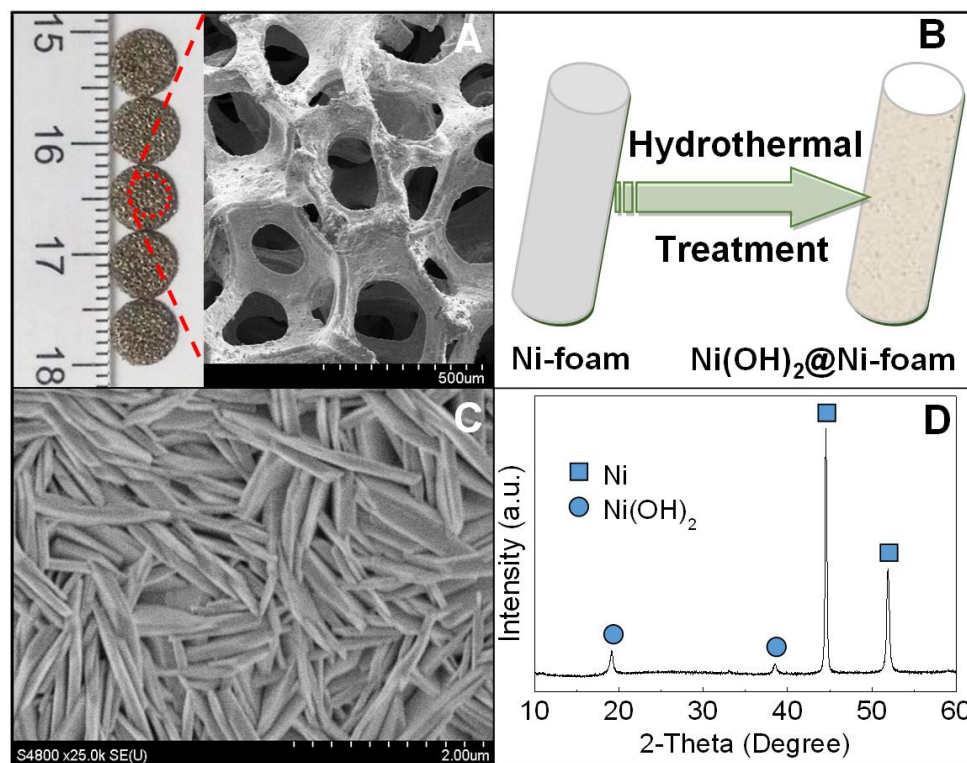
Fig. S12. (A) Photograph of macroscopic samples (left) and low-magnification SEM image (right) of the original monolithic structured Ni-foam with open 3D macroporous network. (B) Scheme of the preparation of Ni(OH)$_2$/Ni-foam substrate by hydrothermal treatment at 100 ^{o}C for 3 h. (C) SEM image of Ni(OH)$_2$/Ni-foam with Ni(OH)$_2$ nano-sheets covering Ni-foam. (D) XRD pattern of the as-prepared Ni(OH)$_2$/Ni-foam substrate.
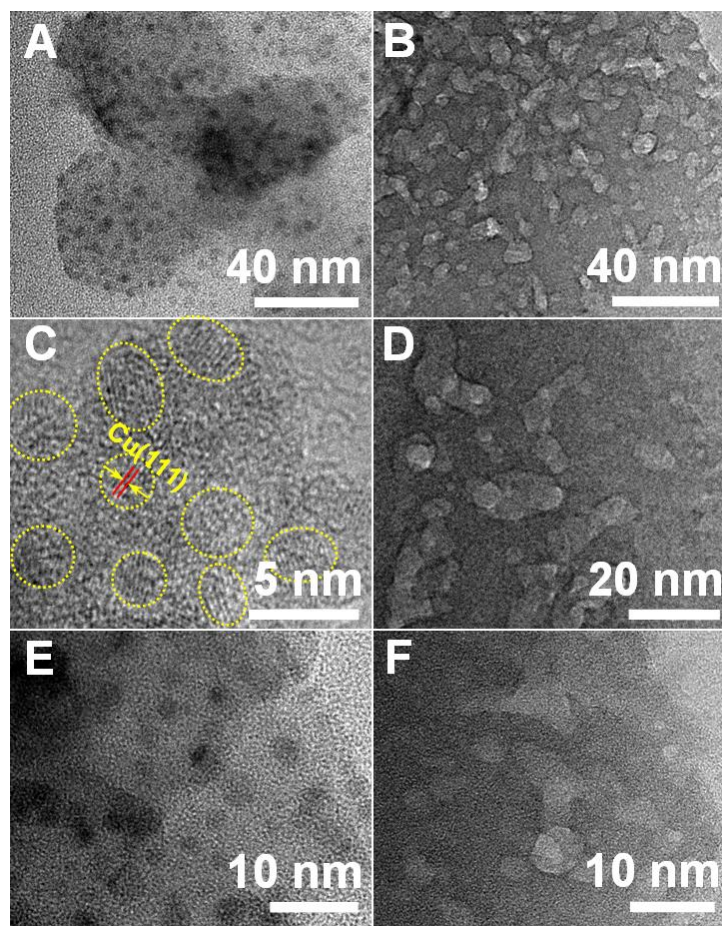
Fig. S13. TEM images of the fresh (A,B) Au@SiO_2/Al_2O_3/Al-fiber, (C,D) Cu@ZrO_2/NiO/Ni-foam and (E,F) NiO@TiO_2/Al_2O_3/Al-fiber catalysts. (B,D,F): TEM images of the samples treated with HNO_3 solution, showing uniform nano-holes, confirming the embedment of metal nanoparticles into the oxides matrix.

Note for Fig. S13C: Because the contrast level of Cu is very close to that of ZrO_2, the Cu-cores in ZrO_2-shell can't be distinguished by their difference in contrast level. Therefore, Cu-cores were picked out with the aid of the lattice fringes, and marked in the dashed circles.
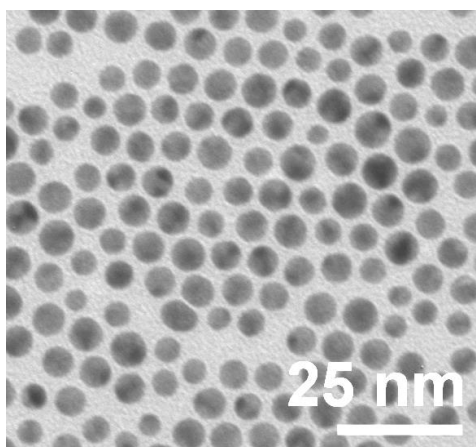
Fig. S14. TEM image of the Au NPs prepared according to the reported method.[S6]

References

S1   C. Wang, L. Han, Q. Zhang, Y. Li, G. Zhao, Y. Liu, Y. Lu, *Green Chem.*, 2015, **17**, 3762.

S2   G. Zhao, H. Hu, M. Deng, M. Ling, Y. Lu, *Green Chem.*, 2011, **13**, 55.

S3   (a) A. Budakoti, M. Abid, A. Azam, *Eur. J. Med. Chem.*, 2006, **41**, 63; (b) N. V. Kramareva, A. Y. Stakheev, O. P. Tkachenko, K. V. Klementiev, W. Grünert, E. D. Finashina, L. M. Kustov, *J. Mol. Catal., A*, 2004, **209**, 97.

S4   X. Sun, W. Wei, *Langmuir*, 2010, **26**, 6133.

S5   Z. Shi, W. Jiao, L. Chen, P. Wu, Y. Wang, M. He, *Microporous Mesoporous Mater.*, 2016, **224**, 253.

S6   X. Wang, J. Zhuang, Q. Peng, Y. Li, *Nature*, 2005, **437**, 121.